Comparative Study on $In_{0.15}Ga_{0.85}As$,InP, and Si/SiO_2 n-MOSFETs through Monte Carlo Analysis

Yousfia LAIDOUNI [*1], Choukria SAYAH [1], Benyounes BOUAZZA [2], Souheyla FEROUANI [1]

[1]Smart Structures Laboratory (SSL), Department of Electronic and Telecommunications, University of Aïn Temouchent. PO Box 284, 46000, Algeria.

[2]Research Unit of Materials and Renewable Energies, Department of Electronic and Electrical Engineering,University of Abou-BakrBelkaid, Tlemcen, Algeria.

*Corresponding Authors: yousfia.laidouni@univ-temouchent.edu.dz ; laidouni.yesm@yahoo.fr

Received: 02-10- 2023 **Accepted:** 08-12-2023 **Published**:15-12- 2023

Abstract

The present study aims to carry out a theoretical investigation on the electronic transport properties of nanometer-scale metal-oxide semiconductor field-effect transistor (MOSFET) devices based on Si and various III–V compounds, using the Monte Carlo method and considering the quantum effects. In this regard, the electronic transport properties of InP-based MOSFET and Si-based MOSFET were assessed and compared with results previously published for transistors based on the same materials and having the same gate length. Afterwards, the advantages of a MOSFET device made of an $In_{0.15}Ga_{0.85}As$ compound semiconductor as new channel material, and a high-k gate dielectric oxide layer (Al_2O_3), were explored. All calculations were carried out at the temperature T = 300° K, using finite element Monte Carlo simulations which incorporate quantum corrections and accounting for scattering mechanisms, such as polar optical phonons, non-polar optical phonons, acoustic phonons, and inter-valley phonons. Local magnitude quantities, such as the electric field, speed of carriers and their energies in MOSFET transistors with nano-metric gate length, were also analysed.

Keywords: III–V compounds, ballistic transport, MOSFET device, diffusion mechanisms, Quantum effects.

*Tob Regul Sci.™ 2023 9(2):*1771 - 1782

DOI: doi.org/10.18001/TRS.9.2.111

Introduction

The field of wireless communications has witnessed rapid growth as a result of the significant advancements in analog radio frequency (RF) technologies. This progress heavily relies on the evolution and improvement of integrated circuits with regard to performance, physical size, and production costs. It was revealed that when the geometry of the device decreases, its sensitivity to environmental factors, like electromagnetic waves and nuclear radiation, increases [1]as the

device becomes more susceptible to defects in the constituting materials [2]. In order to deal with these challenges, it was deemed more appropriate to replace conventional silicon with III-V compounds which have recently emerged as promising materials that are inclined to be increasingly employed for the development of new devices with outstanding electronic transport properties [3]–[5]. It has been reported that the use of high-k metal gate technology compatible with III-V materials can contribute to achieving significant improvements in the insulated gate architecture, particularly in grid control. It has also been revealed that reducing the gate length to 25 nm can result in lower electron mobility and drift velocity, which makes it more challenging to achieve the desired ballistic and near-ballistic transport regime [4]. Moreover, it would not have been possible to attain these great accomplishments without relying on the modeling of the physical phenomena that govern the component's operation. The models are expected to keep up with technological advancements; they must enable the evaluation of all potential enhancements that may result from the use of new techniques. Within this framework, the Monte Carlo (MC) method has become a valuable tool for investigating carrier transport in ultra-small devices like MOSFETs based on III-V compounds [3], [6], [7] . This approach involves monitoring and tracking the specific movements of charge carriers within a crystal to calculate the mean values and determine the macroscopic properties of the system [3].

Nonetheless, in Nano scale MOSFET devices, some quantum effects may occur within the channel along the normal direction of the oxide interface [8]–[10]. In this context, several device simulation approaches, in which transport is managed quantum mechanically, have emerged in recent years [11]. Previously, the coupling of the Schrödinger and Poisson equations has been used in many studies for the purpose of determining the load's real position and any mobility changes [9], [12], [13]. An efficient potential approach, where the quantum mechanical effects were integrated into the MC method [6], [14], while considering a potential quantum correction in the equations of motion [15], [16], was subsequently developed in order to eliminate the need for a complete solution of the Schrödinger equation and consequently avoid additional calculations and save simulation time [9], [15].

In our study, we utilize an Ensemble Monte Carlo method coupled with solving the Poisson equation and incorporating an effective potential to accommodate quantum effects.

The focus of our study lies in the detailed analysis of a metal-oxide-semiconductor field-effect transistor (MOSFET) device based on $In_{0.15}Ga_{0.85}As$. Our primary goal is to explore the intricate physical parameters of a submicron device. We aim to assess the potential advantages offered by new channel materials, taking into meticulous consideration diffusion effects and quantum mechanical phenomena. Throughout this examination, a critical aspect of our research involves ensuring the preservation of the mobility and drift velocity of electrons within the channel, thereby providing a comprehensive understanding of the device's behavior under varying conditions.

1. Model Used

Two-dimensional (2D) simulations of n-channel MOSFET based on $In_{0.15}Ga_{0.85}As$ discussed in the following sections were carried out using a finite element MC device simulation tool in witch Quantum corrections have been incorporated.

1.1. Self-Consistent Monte Carlo Method

The MC method is applied to simulate non-equilibrium particle dynamics in semiconductor materials and devices by solving the Boltzmann Transport Equation (BTE) [17], [18].

This is a quite suitable approach used for the analysis of transport of bulk materials as it generally tracks the movement of carriers in a momentum space [17]. It should be emphasized that in the Boltzmann semi-classical approach, carriers are considered as particles with zero size and following clearly defined trajectories. In addition, the behavior of carriers is represented as a series of free flights and collisions under the action of a constant electric field for a randomly generated time called time of flight [17]. While each particle is simulated as a classical particle during its flight, quantum physics determines the duration of free flights, collisions, and states after collision. The movements of carriers are usually described as a succession of free flights interspersed with instantaneous interactions with the crystal lattice.

The free flight sequence is repeated until the simulation end time is reached and the free flight ends with a scattering event [17]. It is important to mention that the free flight duration depends on the total diffusion rate which is the sum of the diffusion rates of each individual diffusion source [3]. In general, there are two distinct processes that are used to describe the evolution of carriers in a system, the mean free paths ($l\varphi$) and the scattering [3], [17].

The conduction band is approximated by a non-parabolic dispersion relation, which relates the wave vector to the energy of the Γ, L, and X valleys [3]as given in the following form:

$$\varepsilon\left(1+\alpha_i\varepsilon\right)=\frac{\hbar^2k^2}{2m_i^*} \tag{1}$$

- $\alpha_i$isthe coefficient of non-parabolicity of the considered valley
- k: is the pseudo-wave vector
- m_i^* : is the mass of the electron at the minimum of the valley “i” considered
- $\mathcal{E}$and$\hbar$: are respectivelythe energy and the reduced Planck Constant.

During the free flights between collisions, the group velocity v with which the carrier moves is given when integrating the equation of motion by the form (2) [3], [19]–[21]:

$$v = \frac{dr}{dt} \tag{2}$$

More information about the method will be found in reference[18].

For precise device simulations, the electrostatic potential is a required quantity and it can be achieved through the utilization of the Poisson equation. This equation is a fundamental component of Maxwell's equations, which outline the dynamics of the electromagnetic field. The Poisson equation illustrates the evolution of potential due to alterations in charge density, and is identified by its specific formula number as:

$$\nabla^2\varphi = -\frac{\rho}{\varepsilon_S} \tag{3}$$

Here ε_S represents the semiconductor material's dielectric constant, ρ is the total charge density, and φ is the potential.

This makes the Monte Carlo method a semi-quantum technique for semiconductor devices [22] self-consistently simulating the carrier movement classically and carrier scattering quantum-mechanically coupled with solutions of the Poisson equation [17], [22], [23].

1.2. Quantum Effective Potentials

As semiconductor devices undergo further miniaturization, their dimensions approach a scale where they begin to be comparable to the size of an electronic wave packet. In this miniaturized context, quantum effects manifested significantly within the channel region of MOSFET devicesthrough the emergence of a quantum force that can be determined using the carrier concentration at the semiconductor-oxide interface. It may be derived from the Bohm quantum potential Q_B[24]. The Bohm potential is expressed mathematically by the equation n° 4:

$$Q_B = -\frac{\hbar^2}{2\,m^*}\frac{\nabla^2 n}{n} \tag{4}$$

Where n is the magnitude of the wave function.

Efficient potential models have been developed to simulate specific quantum effects arising from the finite size of electronic wave packets. Within this domain, it has been documented that the Monte Carlo ensemble technique, which operates without assuming any distribution function, offers a viable approach to exploring carrier transport involving diverse scattering processes. This approach becomes particularly effective if appropriate quantum effects are incorporated [11]. Achieving this incorporation involves introducing a quantum potential term into the classical electrostatic potential experienced by the simulated particles through the Poisson equation (3).

So, the classical potential is computed using the Poisson equation (3), and the selected effective potential is then added. Subsequently, the transport behavior of electrons is derived from the

calculated potential, providing a comprehensive understanding of their movement within the given system.

$$Q_{quant} = \frac{1}{\sqrt{2\pi\alpha}} \int_{R^n} \varphi_{cl}(x+\xi,t)\ exp\ (-\frac{\xi^2}{2\alpha^2})\ d\xi \quad (5)$$

Where φ_{cl} represent the classical electrostatic potential, n is the dimension of the spatial space, and αcan represent the quantum mechanical "size" of the particle and it is expressed by the from (6) [25]:

$$\alpha = \eta/\sqrt{8m^* k_B T} \quad (6)$$

m^* is the effective mass, k_B is the Boltzmann constant and T is the lattice temperature.

1.3. Implementation

The preceding effective potential method has been incorporated into simulations of n-MOSFETs, where transport was handled using a Monte Carlo approach, employing an isotropic and non-parabolic energy band. The calculations were conducted using the three-valley model (Γ, L, X) and included electron scattering from lattice phonons. The interactions considered in this calculation are due to polar optical phonons, non-polar optical phonons, inter-valley phonons, and acoustic deformation potential.

Boundary conditions assume paramount significance, especially in the domain of sub micrometer devices, wherein contact properties exert a thoughtful influence on the overall behavior of the device [13]. Therefore, in order to avoid the influence of contact properties on the whole behavior of the device, appropriate boundary conditions must be well-defined[26].

When configuring the geometry and the discretization scheme for simulations of behavior, it is important to take into account the plasma frequency and Debye wavelength parameters. It is imperative that the duration of the time steps must be significantly smallerthan the reciprocal value of the plasma frequency, while concurrently ensuring that the mesh dimensions remain shorter than the Debye wavelength[26].

$$L_D = \sqrt{\frac{\mathcal{E}k_B T}{q^2 N}} \approx 42\ \mathring{A} \quad (7)$$

The form (7) expressed the Debye length, where N is the doping density, k_B is the Boltzmann constant and T is the temperature.

- Charge assignment -Every individual particle is meticulously allocated to a specific mesh point. Given the inherent limitations associated with simulating the entirety of electrons within an authentic device, each simulated particle serves as a representative entity embodying a cloud of electrons. This representation is instrumental in approximating currents, charge densities, and

electric field distributions. For all other contexts, it is imperative to note that each discrete particle carries its fundamental charge denoted as e. Furthermore, the incorporation of doping charge is executed in accordance with its designated spatial distribution, thereby enhancing the fidelity of the mesh model.

- It is important to highlight that the initial assumption considers that all particles are in thermal equilibrium. A fixed time step of 1.5 fs is employed, which is considerably shorter than the relaxation time caused by diffusion.
- Mesh size has been selected by (Δx = 1.5 nm, Δy = 0.4 nm).

2. Results and Discussion

The structure employed is an n-MOSFET with L_{ch} = 45 nm as a channel length. The longitudinal dimension (x length) of the device is about 125 nanometers, whereas the overall y length of the entire structure is 100 nanometers.

The left and right contacts were both classified as INSULATORs, functioning as a reflective barrier to prevent particle ingress or egress through these interfaces within the structure.

The Source and Drain contacts were intentionally doped at a concentration of 2×10^{19} cm^{-3} to adhere to the intrinsic constraints imposed by the solid solubility limits of the donors [27]. These contacts were characterized as OHMIC contacts, facilitating the ingress and egress of electrons in and out of the device.

In all calculations, the system was assumed to operate at a temperature of 300 Kelvin. The gate voltage was held constant at Vg = 0.8 V, while the drain voltage was varied from 0.3 V to 0.9 V.

Figure 1 shows the simulated longitudinal electric field characteristics of the Si/SiO_2, InP/ Al_2O_3, and $In_{0.15}Ga_{0.85}As /Al_2O_3$ MOSFETs considered in this study.

The electric field on the drain side has an extremely important negative peak for the three MOSFETs. We notice that for the $In_{0.15}Ga_{0.85}As$ based MOSFT, the magnitude of the longitudinal electric field is greater than in the InP and the Si-based MOSFETs. On the source side, we notice a field peak with a positive value thus indicating the quasi-ballistic acceleration of the electrons and their acquisition of high speeds and their acceleration over a short distance from the source.

This same figure indicates that when the drain voltage increases (> 0.3 V), the absolute peak value of the longitudinal electric field near the source and at the drain increase. It is also noticed that the negative field values at the drain of the $In_{0.15}Ga_{0.85}As$-based MOSFET are lower than those of the InP-based and Si-based MOSFETs. Notably, at the source, the electric field on the drain side demonstrates a significant prominence.

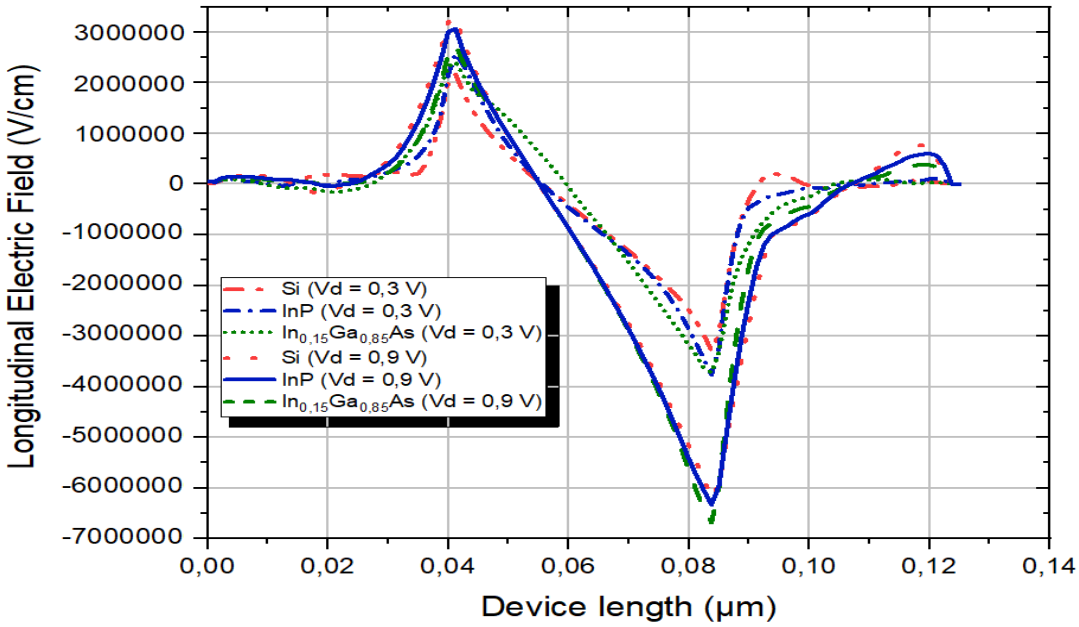

Figure 1. Longitudinal electric fields as a function of x-position in simulated MOSFETs for drain voltages of (Vd = 0.3 V and V_d = 0.9 V) at 300K

Figure 2 presents the results obtained by the quantum-corrected Monte Carlo device simulation. The variations of energies were compared according to the position of the three devices. Notably, it is apparent that, in the case of the $In_{0.15}Ga_{0.85}As$-based MOSFET, electrons at Vd = 0.9 V exhibit higher energy levels compared to the other MOSFETs.

It is observed that, at a drain voltage (Vd) of 0.3 V, the energy curves across the channel display a relatively constant trend for all devices. This suggests a consistent energy distribution at this lower voltage level.

However, as the drain voltage is increased to Vd = 0.9 V, a discernible pattern emerges. The average electron energy exhibit an incremental trend, manifesting distinct peaks across the majority of devices. Notably, in the specific case of the $In_{0.15}Ga_{0.85}As$-based MOSFET, it is noteworthy that electrons at Vd = 0.9 V attain higher energy levels compared to their counterparts in other MOSFETs. The pronounced surge in energy is discerned in proximity to the drain region, attributable to a heightened electric field. Under the influence of this electric field, electrons traverse a considerable real-space distance until reaching their maximum velocity in the K-space.

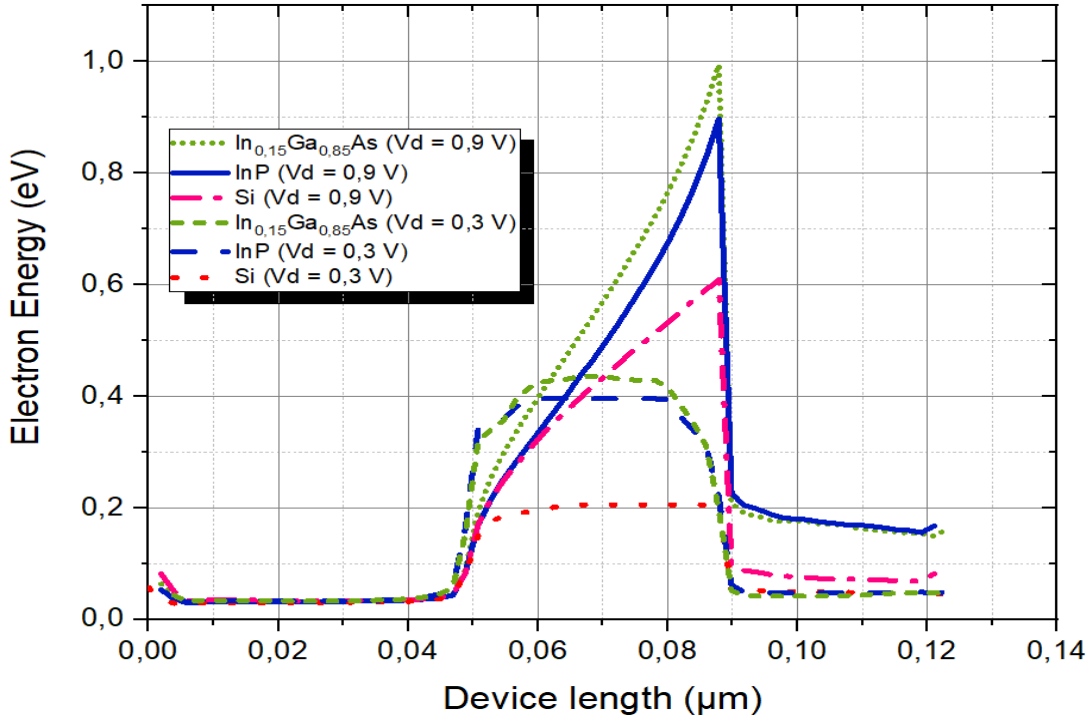

Figure 2. Electron energy distribution across in simulated MOSFETs, for various Drain voltages (Vd=0,3V and Vd = 0.9 V), at 300K.

The occurrence of the maximum kinetic energy in the transistors is notably deep into the drain side, implying a significantly enhanced injection velocity [28]. The distinction in electron energy characteristics at elevated drain voltages may signify unique electronic properties inherent to the $In_{0.15}Ga_{0.85}As$ -based MOSFET. Further analysis is warranted to elucidate the underlying factors contributing to this observed difference in electron behavior under varying drain voltages.

Likewise, Figure 3 depicts the profiles of the electron velocities as a function of distance, for the three simulated devices. The drain voltage Vd = 0.3 V was applied, and the average electron velocity rates were then compared.

It was observed that there is no overshoot phenomenon in the channel area whether for the Si, the InP, or the $In_{0.15}Ga_{0.85}As$-based MOSFETs, which justifies the absence of excess electrons in that zone.

Once the drain voltage climbed to 0.9 V, an overshoot phenomenon is observed along the channel zone for the Si-based MOSFET. Additionally, it is noteworthy that the average velocity increases in the InP-based MOSFET and $In_{0.15}Ga_{0.85}As$-based MOSFET, with the occurrence of a peak in the active region. The position of the peak shifts towards the drain, which implies that a large number of electrons near the drain acquire enough energy to migrate towards the L valley. It is also noted that, for the same drain voltage (0.9 V), the velocity of electrons in the $In_{0.15}Ga_{0.85}As$-based MOSFET is greater than that found in the InP-based MOSFET.

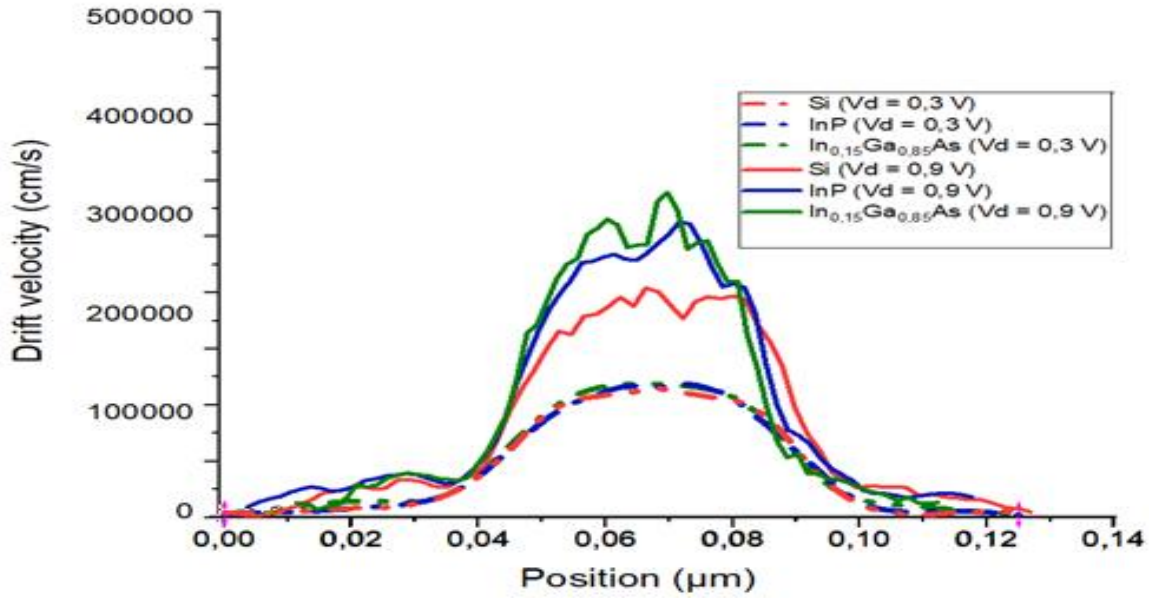

Figure 3.Velocity profile according to the distance in the simulated devices at 300°K for applied voltages; Vg = 0.8 V, Vd = 0.3 V and Vg = 0.8 V, Vg = 0.9 V

Figure 4. represents the electron density profiles. W note that this density deviates significantly from the interface if the drain voltage is maintained at 0.3 V, then the channel remains uninterrupted from the source to the drain. Conversely, for a drain bias potential of 0.9 V, the channel exhibits an evident constraint and is distinctly pinched due to saturation effects. In addition, it is noteworthy that the peak representing the density is tempered due to energy quantization coupled with a higher threshold voltage. Furthermore, the charge carriers tend to localize more outside the interface.

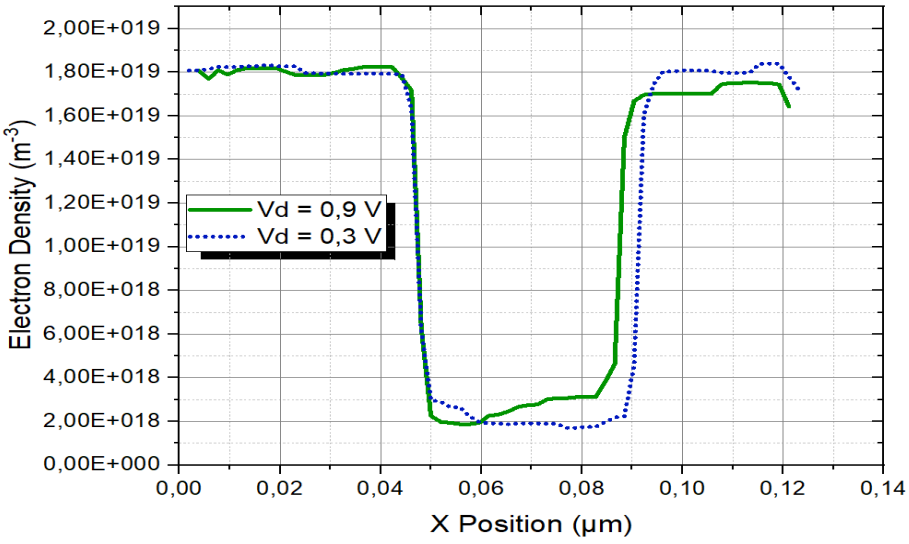

Figure 4. Electron density as versus distance for $In_{0.15}Ga_{0.85}As$ based MOSFET for applied voltages; Vg = 0.8 V, Vd = 0.3 V and Vg = 0.8 V, Vd = 0.9 V.

.3. Conclusion

An ensemble Monte Carlo simulation incorporating quantum effects has been employed to investigate electron transport properties in a Si and III-V-based MOSFET devices.

We have adopted $In_{0.15}Ga_{0.85}As$ as a novel channel material and Al_2O_3 as a high-k dielectric layer, replacing replacing Si- SiO_2 based MOSFET, InP-Al_2O_3 MOSFET and subjecting them to a comparison. Our findings have demonstrated that the transverse electric field, average electron velocity, and mean electron energy in the $In_{0.15}Ga_{0.85}As$ -based MOSFET surpass those in the Si-based MOSFET across all regions of the channel. However, a comparative analysis of Si, InP, and $In_{0.15}Ga_{0.85}As$-based MOSFETs reveals disparate behaviors in various regions and under different voltages.

The outcomes of the study indicated that the method used can provide valid wherewithal to incorporate quantum corrections into device simulations. These results turned out to be in good agreement with those reported in reference [27].

For a high drain voltage, the electrons accumulate close to the latter in the channel for MOSFETs based on InP and $In_{0.15}Ga_{0.85}As$.

The average electron velocity and the average kinetic energy are significantly higher in equivalent $In_{0.15}Ga_{0.85}As$

MOSFET compared to the other simulated devices. This heightened performance persists despite a portion of electrons transferring from the Γvalley with a low effective electron mass to the L and X valleys with higher effective electron masses in the source/drain regions. This phenomenon is attributed to a substantial proportion of electrons consistently being injected into the channel from the Γvalley, resulting in an overall reduction in electron scattering.

Acknowledgment

The authors would like to thank all the technical staff of the Intelligent Structures Laboratory (SSL), University of Aïn Temouchent. PO Box 284, 46000, Algeria for their kind assistant.

References

[1] C. Detcheverry, “Étude du basculement induit par un ion lourd dans une mémoire statique en technologie submicronique.” Montpellier 2, 1997.

[2] E. Cassan, S. Galdin, P. Dollfus, and P. Hesto, “Study of direct tunneling through ultrathin gate oxide of field effect transistors using Monte Carlo simulation,” *J. Appl. Phys.*, vol. 86, no. 7, pp. 3804–3811, 1999.

[3] C. SAYAH, “Etudes-des-Effets-du-Champ-Electromagnétique-sur-les-Propriétés-des-Composés-III-V-par-la-Méthode-de-Monte-Carlo-et-l’Equation-de-Poisson-Couplée,”

Nov. 2013, Accessed: Dec. 14, 2023. [Online]. Available: http://dspace1.univ-tlemcen.dz//handle/112/2991

[4] A. Islam, A. T. Aynul, and K. Kalna, "Analysis of Potential and Electron Density Behaviour in Extremely Scaled Si and InGaAs MOSFETs Applying Monte Carlo Simulations," in *Journal of Physics: Conference Series*, 2020, vol. 1637, no. 1, p. 12007.

[5] J. Lacord, "Développement de modèles pour l'évaluation des performances circuit des technologies CMOS avancées sub-20nm." Grenoble, 2012.

[6] H. Tsuchiya, M. Horino, and T. Miyoshi, "Quantum Monte Carlo device simulation of nano-scaled SOI-MOSFETs," *J. Comput. Electron.*, vol. 2, pp. 91–95, 2003.

[7] C. Sayah, B. Bouazza, A. Guenbouazza, and N.-E. Chabane-Sari, "Etude théorique du transport électronique par la simulation Monte Carlo dans le quaternaire In0. 863Ga0. 137As0. 3P0. 7," *Afrique Sci. Rev. Int. des Sci. Technol.*, vol. 4, no. 2, 2008.

[8] D. K. Ferry, "The onset of quantization in ultra-submicron semiconductor devices," *Superlattices Microstruct.*, vol. 27, no. 2–3, pp. 61–66, 2000.

[9] R. Akis, S. Milicic, D. K. Ferry, and D. Vasileska, "An effective potential method for including quantum effects into the simulation of ultra-short and ultra-narrow channel MOSFETs," in *Proceedings of the 4th International Conference on Modeling and Simulation of Microsystems, Hilton Head Island, SC, March*, 2001, pp. 19– 21.

[10] D. K. Ferry, I. Knezevic, S. M. Ramey, and L. Shifren, "Nonequilibrium Transport in Nanoscale Semiconductor Devices," in *Progress in Nonequilibrium Green's Functions II*, World Scientific, 2003, pp. 127–142.

[11] D. K. Ferry, "Simulation at the start of the new millenium: Crossing the quantum-classical threshold," *VLSI Des.*, vol. 13, no. 1–4, pp. 155–161, 2001.

[12] D. Vasileska, D. K. Schroder, and D. K. Ferry, "Scaled silicon MOSFETs: Degradation of the total gate capacitance," *IEEE Trans. Electron Devices*, vol. 44, no. 4, pp. 584–587, 1997.

[13] D. Vasileska and D. K. Ferry, "The influence of space quantization effects on the threshold voltage, inversion layer and total gate capacitances in scaled Si-MOSFETs," *Nanotechnology*, vol. 10, no. 2, p. 192, 1999.

[14] C. S. Soares, P. K. R. Baikadi, A. C. J. Rossetto, M. A. Pavanello, D. Vasileska, and G. I. Wirth, "Modeling Quantum Confinement in Multi-Gate Transistors with Effective Potential," in *2022 36th Symposium on Microelectronics Technology (SBMICRO)*, 2022, pp. 1–4.

[15] H. Tsuchiya, M. Horino, M. Ogawa, and T. Miyoshi, "Quantum transport simulation of ultrathin and ultrashort silicon-on-insulator metal–oxide–semiconductor field-effect transistors," *Jpn. J. Appl. Phys.*, vol. 42, no. 12R, p. 7238, 2003.

[16] T. Mori, Y. Azuma, H. Tsuchiya, and T. Miyoshi, "Comparative study on drive current of III–V semiconductor, Ge and Si channel n-MOSFETs based on quantum-

corrected Monte Carlo simulation," *IEEE Trans. Nanotechnol.*, vol. 7, no. 2, pp. 237–241, 2008.

[17] G. F. Furtado, V. V. de A. Camargo, D. Vasileska, and G. I. Wirth, "3-D TCAD Monte Carlo device simulator: State-of-the-art FinFET simulation," *J. Integr. circuits Syst. Porto Alegre. Vol. 16, no. 2 (2021), p. 1-10*, 2021.

[18] B. Bouazza, A. Guen-Bouazza, C. Sayah, and N. E. Chabane-Sari, "Comparison of High Field Electron Transport in GaAs, InAs and In0. 3Ga0. 7As," *J. Mod. Phys.*, vol. 4, no. 4, pp. 121–126, 2013.

[19] M. V Fischetti, "Monte Carlo simulation of transport in technologically significant semiconductors of the diamond and zinc-blende structures. I. Homogeneous transport," *IEEE Trans. Electron Devices*, vol. 38, no. 3, pp. 634–649, 1991.

[20] P. Lugli, "MONTE-CARLO SIMULATION OF ULTRAFAST PHENOMENA," *Helv. Phys. ACTA*, vol. 62, no. 6–7, pp. 691–695, 1989.

[21] M. Ogawa, H. Tsuchiya, and T. Miyoshi, "Quantum transport modeling in nano-scale devices," in *International Conference on Simulation of Semiconductor Processes and Devices*, 2002, pp. 261–266.

[22] B. Bouazza, A. Guen-Bouazza, L. Amer, C. Sayah, N. E. Chabane-Sari, and C. Gontrand, "Étude du transport électronique dans le substrat InAs de type N par la simulation de Monte Carlo," *Afrique Sci.*, vol. 1, no. 1, pp. 55–67, 2005.

[23] B. Thorpe, S. Schirmer, and K. Kalna, "Monte Carlo simulations of spin transport in nanoscale transistors: temperature and size effects," *Semicond. Sci. Technol.*, vol. 37, no. 7, p. 75009, 2022.

[24] D. K. Ferry, J. Weinbub, M. Nedjalkov, and S. Selberherr, "A review of quantum transport in field-effect transistors," *Semicond. Sci. Technol.*, vol. 37, no. 4, p. 43001, 2022.

[25] L. Han and C. Wang, "Effect of quantum effects on electrical transport in Si/Ge/Si sandwich structure," in *2011 12th International Conference on Electronic Packaging Technology and High Density Packaging*, 2011, pp. 1–2.

[26] C. Sayah, B. Bouazza, A. Guen-Bouazza, and N. E. Chabane-Sari, "Simulation of electron transport in GaN based MESFET using Monte Carlo method," *World Appl. Program.*, vol. 2, pp. 97–103, 2012.

[27] A. Akbari Tochaei, H. Arabshahi, M. R. Benam, A. Vatan-Khahan, and M. Abedininia, "Comparison between Si/SiO 2 and InP/Al 2 O 3 based MOSFETs," *J. Exp. Theor. Phys.*, vol. 123, pp. 869–874, 2016.

[28] A. Islam, B. Benbakhti, and K. Kalna, "Monte Carlo Study of Ultimate Channel Scaling in Si and In $ _ {\rm 0.3} $ Ga $ _ {\rm 0.7} $ As Bulk MOSFETs," *IEEE Trans. Nanotechnol.*, vol. 10, no. 6, pp. 1424–1432, 2011.